In situ observation of secondary phase formation in Fe implanted GaN annealed in low pressure N_2 atmosphere

G. Talut, J. Grenzer, H. Reuther, A. Shalimov, C. Baehtz, D. Novikov, and B. Walz

Citation: Appl. Phys. Lett. **95**, 232506 (2009); doi: 10.1063/1.3271828
View online: https://doi.org/10.1063/1.3271828
View Table of Contents: http://aip.scitation.org/toc/apl/95/23
Published by the American Institute of Physics

In situ observation of secondary phase formation in Fe implanted GaN annealed in low pressure N_2 atmosphere

G. Talut,[1,a)] J. Grenzer,[1] H. Reuther,[1] A. Shalimov,[1] C. Baehtz,[1] D. Novikov,[2] and B. Walz[2]
[1]*Institute of Ion Beam Physics and Materials Research, Forschungszentrum Dresden-Rossendorf e.V., P.O. Box 510119, 01314 Dresden, Germany*
[2]*Deutsches Elektronen-Synchrotron DESY, Notkestraße 85, 22607 Hamburg, Germany*

(Received 26 October 2009; accepted 16 November 2009; published online 8 December 2009)

The formation of secondary phases in Fe implanted GaN upon annealing in low pressure N_2-atmosphere was detected by means of *in situ* x-ray diffraction and confirmed by magnetization measurements. A repeatable phase change from Fe_3N at room temperature and $Fe_{3-x}N$ at 1023 K was observed *in situ*. The phase transformation is explained by the change of lattice site and concentration of nitrogen within nitrides. The diffusion of Fe toward sample surface and oxidation with increasing annealing cycles limits the availability of secondary phase and hence the repeatability. At high temperature GaN dissolves and Ga as well as Fe oxidize due to presence of residual oxygen in the process gas. The ferromagnetism in the samples is related to nanometer sized interacting $Fe_{3-x}N$ crystallites. © *2009 American Institute of Physics*. [doi:10.1063/1.3271828]

GaN is a wide band gap semiconductor that has been studied intensively in the last years because of its potential field of applications like in optoelectronics, plasmonics, as well as for high power electronics. By doping with transitional metals like Fe it might also be a diluted magnetic semiconductor (DMS) with a Curie temperature above room temperature (RT) and could then be used for spintronics.[1] There are many experimental studies reporting ferromagnetism at RT in Fe doped GaN. In a real DMS, with magnetic atoms randomly substituting cation sites, ferromagnetic coupling is supposed to be due to the indirect exchange coupling between magnetic impurities mediated by holes.[1–4] Experimental observation of strong-coupling effects in a DMS $Ga_{1-x}Fe_xN$ was reported by Pacuski *et al.*[5] Robust ferromagnetism in the region of insulator-to-metal transition was predicted for high hole densities. However, there are also other possible sources of ferromagnetism like spinodal decomposition of Fe or ferromagnetic secondary phases. The detection of those is rather difficult. Bonanni *et al.*[6] prepared GaN:Fe layers by metalorganic chemical vapor deposition (MOCVD) and observed ferromagnetism that was partially accounted to the spinodal decomposition and non-uniform distribution of Fe-rich magnetic nanocrystals. Kuwabara *et al.*[7] reported the formation of nanoclusters and superparamagnetic behavior in GaN:Fe epilayers prepared by rf-plasma-assisted molecular beam epitaxy. In case of ion implantation the reports from different groups are quite controversial. Theodoropoulou *et al.*[8] and Shon *et al.*[9,10] did not relate ferromagnetic response to secondary phases after transition ion implantation into semiconductors. In our experiments, however, the formation of α-Fe nanoclusters, that were responsible for ferromagnetic response, was observed.[11] Though the appearance of such precipitates is not desired in a DMS they might be useful for certain applications.[12] Li *et al.*[13] detected co-occurrence of α-Fe and ε-Fe_3N in MOCVD prepared GaN:Fe films and pointed out the role of nitrogen pressure and structural disorder in the formation of Fe-rich phases. Bonanni *et al.*[14] have shown that the controlled aggregation of magnetic ions in a semiconductor can be affected by the growth rate and doping with shallow impurities.

Recently we reported predominant formation of epitaxially oriented α-Fe nanoclusters if Fe-doped samples were annealed in a N_2 flow at 1.1 bar pressure.[11] In this paper we report the formation of ε-$Fe_{3-x}N$ with $x<1$ that builds up during annealing at 1073 K in 0.5 bar N_2 and the reversible transformation to ε-Fe_3N during cooling down to RT.

P-type (Mg) doped ($\sim 2\times10^{17}$ cm^{-3}) single crystalline wurtzite GaN(001) films of about 3 μm thickness epitaxially grown by metal organic vapor phase epitaxy on sapphire (001) were used. Samples, 7° tilted relative to the ion beam to avoid channeling, were implanted with 195 keV ^{57}Fe ions with fluence $\Phi=4\times10^{16}$ cm^{-2} (peak Fe concentration of 4 at. % at the projected range $R_p=85$ nm according to TRIM[15]), keeping the samples at RT. In order to reduce the implantation damage and to investigate the formation of secondary phases the implanted samples were annealed at 1073 K in a low pressure N_2-atmosphere(0.5 bar) within several minutes. The annealing experiments along with the *in situ* x-ray diffraction characterization were performed at the Rossendorf beamline at the ESRF in Grenoble with a x-ray wavelength of $\lambda=0.124$ nm. The annealing chamber was equipped with a boron nitride heater, controlled by a Eurotherm controller, gas inlet and a half sphere beryllium dome. The temperature was measured by a PtRh/Pt thermocouple placed on top of the heater. The gas pressure in the chamber was limited to 0.5 bar with a flow of about 40 $1\cdot min^{-1}$. The purity of the N_2 gas (99.9999%) was limited by the setup with an oxygen contamination in the ppm range.

A Pilatus 100 K two-dimensional (2D) pixel detector was used to record 2D diffraction pattern. Additionally, a scintillation counter was used for 2θ-ω-scans. Generally, for clusters in the range of some nm the signal to background ratio is very low. In order to increase the signal to background ratio to an acceptable level the acquisition time of the 2D detector was set to 10 s and those of the scintillation counter to 5 s per point. The investigations of the magnetic properties were performed with a Quantum Design MPMS

a)Electronic mail: g.talut@fz-rossendorf.de.

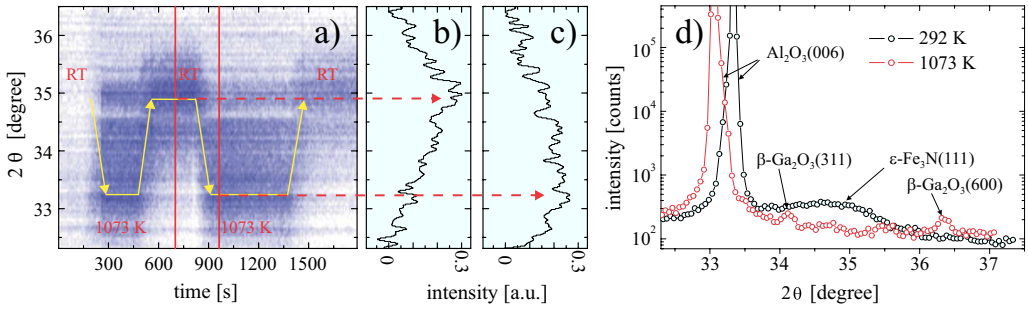

FIG. 1. (Color online) (a) Time dependent 2θ-scans between 32.3° and 36.5° at ω=17.7°. The presentation is based on the line profiles from the 2D detector with an 10 s acquisition time each. Intensity is color/grayscale coded with dark color representing higher intensity. On the right two profiles are presented for the (b) RT and (c) 1073 K scans. (d) 2θ-ω coupled scans at RT and 1073 K recorded after third cycle with a scintillation counter.

superconducting quantum interference device magnetometer. For the evaluation of the 2D detector exposures rectangular areas with dimensions 2θ from 32.3° to 36.5° and $\chi = \pm 0.2°$ (angle $\perp$ to the scattering plane) were integrated over χ and assumed as line scans. Those line scans are represented over annealing/cooling time with the color/grayscale coded intensity in Fig. 1(a). Single examples of line scans are given in Figs. 1(b) and 1(c) for RT and 1073 K, respectively. Prior to the annealing procedure (time t=0 at RT) no reflexes from secondary phases were detected [see Fig. 1(a)]. After about 200 s annealing, at 1073 K, a broad reflex starts to evolve in the region between 32.5° and 35° with a local maximum at about 33.3°. The peak shift due to the lattice expansion from RT to 1073 K is in the order of 0.1° and can be neglected. The position of the maximum fits well to the pattern of FeN(200) (33.46° at RT). However, because of the broadness of the reflex, other nitrides like disordered ε-$Fe_{3-x}N$(002) or ζ-Fe_2N(102) can also be taken into account. Disordered in this sense means the redistribution of mainly N atoms within the structure and can be described by the transfer of N from Fig. 2(b) and 2(c) Wyckoff site position in the ε-$Fe_{3-x}N$-phase.[16] From symmetry reasons the formation of ε-$Fe_{3-x}N$ is more probable since it features the same type of structure (wurtzite) as GaN. The strain caused by the lattice mismatch is supposed to relax by generating misfit dislocations, as was shown in Ref. 13.

During cooling down (t=500 s) from 1073 K to RT the reflex shifts consistently toward higher angular values as represented by arrows. At RT the maximum of the peak ends up at about 34.9° and can be assigned to ε-Fe_3N(111). This is shown in a selected plot at RT in Fig. 1(b). The presence of ε-Fe_3N correspond with the results in Refs. 13 and 14 However the change of symmetry cannot be explained up to now. The mean size of clusters, calculated with Scherrer formula using the full width at half maximum, is about 5 nm. However, the values calculated by means of Scherrer formula should be treated carefully. Because of the weak scattering intensity of the only secondary phase reflex no statement about the microstrain or mosaicity can be made.

The following annealing sequence, starting now from the already formed ε-Fe_3N(111) phase lead to a peak shift from 34.9° at RT to 33.3° at 1073 K; cooling down to RT reverses the phase transformation again. Hence, the process of phase transformation from a partially disordered ε-$Fe_{3-x}N$ to an ordered ε-Fe_3N is reproducible.

The process of secondary phase formation is suggested as follows. After the ion implantation a highly defective GaN with broken Ga–N bonds is present. During annealing in low pressure N_2 atmosphere atomic nitrogen can escape from the surface region leading to a further dissolution of GaN. Considering the energies of formation if atomic nitrogen is available the formation of iron nitrides rather than of GaN is preferable. Once ε-$Fe_{3-x}N$ is formed the transformation between the ε-$Fe_{3-x}N$ and ε-Fe_3N phases occur over the N exchange and lattice site change. In contrast to that, the annealing in a high pressure N_2 atmosphere (at 1.1 bar) prevents the out-diffusion of nitrogen out of the damaged region, thus reducing the dissolution of GaN. In this case bcc-Fe is formed predominantly.

At this point it should be mentioned, that the reversibility is limited by the out-diffusion of Fe and gradual oxidation of Fe and Ga. During annealing the reflex intensities of the secondary phases decreases and after some repetitions reflexions from nitrides disappeared completely. This can be seen in Fig. 1(d), that shows two coupled 2θ-ω line scans recorded with the scintillation counter at RT after first annealing cycle and at 1073 K during the third annealing cycle. The shift of Al_2O_3 is due to its thermal expansion and is consistent with Ref. 17 this confirms proper temperature control. The additional small reflexes in the 1073 K spectrum are related to the β-Ga_2O_3 reflexes. The full set of β-Ga_2O_3 reflexes was found in this sample (not shown), referring to the polycrystallinity of the oxide layer.[18]

Magnetic measurements were performed on the samples in virgin and as implanted state, then after annealing at 1073 K for one cycle and after three cycles annealing accordingly. Virgin as well as implanted samples show no ferromagnetic response. The sample annealed for one cycle show a characteristic behavior of superparamagnetic nanoparticles. Figure 2 shows a zero-field-cooled/field-cooled (ZFC/FC)

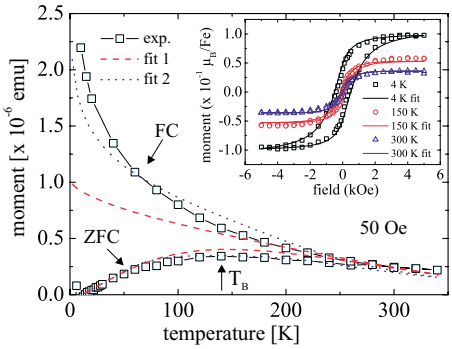

FIG. 2. (Color online) ZFC/FC measurement performed at 50 Oe on the sample implanted with 3×10^{16} cm^{-2} and annealed at 1073 K for one cycle along with the fitting results using Preisach model. The inset shows magnetization curves recorded at 4, 150, and 300 K.

measurement along with the magnetization curves (inset) of this sample recorded at 4, 150, and 300 K. The broad maximum in the ZFC part of the curve gives a hint of a large size distribution of the nanoparticles with the mean blocking temperature T_B of about 130 K. Using a formalism for the relaxation time τ of the particle magnetization with the anisotropy energy density E_A (2×10^4 J/m^3),[19] the attempt frequency f_0 (typically 10^9–10^{11} Hz), measurement time 100 s, Boltzmann constant k_B the volume V of the mean sized cluster can be calculated. From that a diameter of about 16 nm is estimated, assuming a spherical shape of clusters

$$\tau^{-1} = f_0 \cdot \exp\left(-\frac{E_A V}{k_B T_B}\right). \quad (1)$$

However, the blocking temperature may be influenced by magnetic interactions between the particles.[6] This can lead to an overestimation of cluster size. A Preisach model was applied to fit the ZFC/FC as well as the magnetization loops.[20,21] The model assumes the decomposition of magnetic system into an ensemble of bistable units characterized by a temperature dependent spontaneous moment μ, two possible magnetic states $\pm\mu$, and two characteristic values of coercive h_c and asymmetry h_i fields. Best fitting results were obtained by using Lorentz type functions for the coercive and asymmetry field distributions. The average spontaneous moment of the clusters at 0 K μ_0, mean coercive field h_{c0}, power law temperature dependence parameter σ_c and σ_i as well as the critical temperature T_c were best fitted using $\mu_0=7.7\times10^{-16}$ emu ($\cong8.3\times10^4$ μ_B), $h_{c0}=150$ Oe, $\sigma_c=800$ Oe, $\sigma_i=900$ Oe, and $T_c=480$ K, respectively (fit 1). With 1.9 μ_B/Fe for the magnetic moment of Fe in ε-Fe_3N (Ref. 22) and 3 Fe atoms in a unit cell the number of unit cells and out of it the cluster volume can be calculated. Again, assuming the spherical shape of the cluster its diameter can be calculated to about 9 nm. This model describes the ZFC curve as well as the hysteresis loops very precise. An indication of superparamagnetic behavior of clusters is the breakdown of the coercive field with increasing temperatures (see inset in Fig. 2). It has to be noted that the moment per Fe atom in μ_B is by a factor 20 lower than of pure ε-Fe_3N.[16] This means that not all Fe are incorporated in the formation of ε-Fe_3N. Unfortunately, the mean size cluster approach is not able to describe the enhanced magnetization in the FC curve at low temperatures, related to the response from those magnetic clusters which are larger than 9 nm. Using two mean moments $\mu_0=7\times10^{-16}$ and 14×10^{-16} emu ($\cong$ mean sizes 9 and 11 nm) and different cluster concentrations the fit approaches the experimental curve (fit 2). This bimodal size distribution hint that clusters are in a coalescent regime, since the volume of a 11 nm sized cluster is close to the volume of two merged 9 nm sized clusters.

After annealing for three cycles at 1073 K no ferromagnetic response was detected. Because of the oxidation of Ga as well as of Fe the layer can be regarded as Ga_2O_3 with inclusions of some iron oxide. This result is in contrast to the results from Lee *et al.*,[23] where Fe doped β-Ga_2O_3 was found to be ferromagnetic.

In summary, reversible phase transition of Fe implanted GaN was observed upon annealing in 0.5 bar N_2 at 1073 K by means of *in situ* x-ray diffraction and discussed in terms of N exchange. After annealing ε-Fe_3N was found to be formed predominantly and is responsible for ferromagnetic response. It demonstrates that by variation of annealing conditions specific secondary phases can be created, leading to different electronic, magnetic and other properties. Preisach model yields an reasonable estimation of magnetic quantities and cluster size. The cluster size is in a good agreement with the calculation using Scherrer formula. No DMS related phenomena have been observed.

The annealing process is accompanied by a strong diffusion of N and dissolution of GaN, mediated by the formation of nitrides and oxides. Oxygen contamination further promotes the dissolution of GaN and the formation of β-Ga_2O_3. Hence, it acts as a further limiting aspect and need to be excluded in the following experiments. Fe doped β-Ga_2O_3 was found to be paramagnetic which is in contrast with the findings in Ref. 12.

G. Talut acknowledges the Deutsche Forschungsgemeinschaft (German Research Foundation) for the financial support under Contract No. Re 868/8-2.

[1] T. Dietl, H. Ohno, and F. Matsukura, Phys. Rev. B **63**, 195205 (2001).
[2] K. Sato and H. Katayama-Yoshida, Jpn. J. Appl. Phys., Part 2 **40**, L485 (2001).
[3] K. Sato and H. Katayama-Yoshida, Semicond. Sci. Technol. **17**, 367 (2002).
[4] T. Dietl, Phys. Rev. B **77**, 085208 (2008).
[5] W. Pacuski, P. Kossacki, D. Ferrand, A. Golnik, J. Cibert, M. Wegscheider, A. Navarro-Quezada, A. Bonanni, M. Kiecana, M. Sawicki, and T. Dietl, Phys. Rev. Lett. **100**, 037204 (2008).
[6] A. Bonanni, M. Kiecana, C. Simbrunner, T. Li, M. Sawicki, M. Wegscheider, M. Quast, H. Przybylińska, A. Navarro-Quezada, R. Jakieła, A. Wolos, W. Jantsch, and T. Dietl, Phys. Rev. B **75**, 125210 (2007).
[7] S. Kuwabara, T. Kondo, T. Chikyow, P. Ahmet, and H. Munekata, Jpn. J. Appl. Phys., Part 2 **40**, L724 (2001).
[8] N. Theodoropoulou, A. F. Hebard, S. N. G. Chu, M. E. Overberg, C. R. Abernaty, S. J. Pearton, R. G. Wilson, and J. M. Zavada, J. Appl. Phys. **91**, 7499 (2002).
[9] Y. Shon, Y. H. Kwon, Y. S. Park, Sh. U. Yuldashev, S. J. Lee, C. S. Park, K. J. Chung, S. J. Yoon, H. J. Kim, W. C. Lee, D. J. Fu, T. W. Kang, X. J. Fan, Y. J. Park, and H. T. Oh, J. Appl. Phys. **95**, 761 (2004).
[10] Y. Shon, S. Lee, H. C. Jeon, Y. S. Park, D. Y. Kim, T. W. Kang, J. S. Kim, E. K. Kim, D. J. Fu, X. J. Fan, Y. J. Park, J. M. Baik, and J. L. Lee, Appl. Phys. Lett. **89**, 082505 (2006).
[11] G. Talut, H. Reuther, S. Zhou, K. Potzger, F. Eichhorn, and F. Stromberg, J. Appl. Phys. **102**, 083909 (2007).
[12] S. Zhu, Y. Li, C. Fan, D. Zhang, W. Liu, Z. Sun, and S. Wei, Physica B **364**, 199 (2005).
[13] T. Li, C. Simbrunner, A. Navarro-Quezada, M. Wegscheider, M. Quast, D. Litvinov, D. Gerthsen, and A. Bonanni, J. Cryst. Growth **310**, 3294 (2008).
[14] A. Bonanni, A. Navarro-Quezada, M. Tian, L. Wegscheider, Z. Matěj, V. Holý, R. T. Lechner, G. Bauer, M. Rovezzi, F. D'Acapito, M. Kiecana, M. Sawicki, and T. Dietl, Phys. Rev. Lett. **101**, 135502 (2008).
[15] Part of the SRIM program package by J. F. Ziegler at http://www.srim.org/.
[16] A. Leineweber, H. Jacobs, F. Huning, H. Lueken, H. Schilder, and W. Kockelmann, J. Alloys Compd. **288**, 79 (1999).
[17] G. Fiquet, P. Richet, and G. Montagnac, Phys. Chem. Miner. **27**, 103 (1999).
[18] K. H. Jack, Proc. R. Soc. London, Ser. A **208**, 200 (1951).
[19] R. S. Ningthoujam and N. S. Gajbhiye, Mater. Res. Bull. **43**, 1079 (2008).
[20] T. Song, R. M. Roshko, and E. Dan Dahlberg, J. Phys.: Condens. Matter **13**, 3443 (2001).
[21] A. Shalimov, K. Potzger, D. Geiger, H. Lichte, G. Talut, A. Misiuk, H. Reuther, F. Stromberg, S. Zhou, C. Baehtz, and J. Fassbender, J. Appl. Phys. **105**, 064906 (2009).
[22] J. M. Gallego, S. Yu. Grachev, D. M. Borsa, D. O. Boerma, D. Écija, and R. Miranda, Phys. Rev. B **70**, 115417 (2004).
[23] S. W. Lee, Y. G. Ryu, G. Y. Ahn, S. -I. Park, and C. S. Kim, Phys. Status Solidi C **1**, 3550 (2004).